Jurnal Kejuruteraan 32(4) 2020: 715-721
https://doi.org/10.17576/jkukm-2020-32(4)-22

An Improved Efficiency by Surface Modification Using Pulse Laser for Partial Transparent Bifacial Solar Cell

Muhd Hatim Rohaizar, Suhaila Sepeai*, Norasikin Ahmad Ludin, Mohd Adib Ibrahim, Kamaruzzaman Sopian & Saleem H.Zaidi
Solar Energy Research Institute (SERI)
Universiti Kebangsaan Malaysia, 43600 UKM Bangi Selangor, Malaysia

**Corresponding author: suhailas@ukm.edu.my*

Received 17 September 2019, Received in revised form 29 October 2019
Accepted 10 January 2020, Available online 30 November 2020

ABSTRACT

Bifacial solar cell has symmetrical configuration contacts on front and rear surface that eliminate expansion mismatch, decrease metal usage and improves photon absorption. The limitation of the reflector at the back of bifacial solar panel able to be eliminated by developing special designed partially transparent bifacial solar cell to optimize light trapping on rear surface. Therefore, the partial transparent silicon (Si) wafers were developed to increase light transmission to rear surface. Surface modification on Si wafer was conducted to form partial transparent Si wafer. Surface modification was employed by pulsed laser interaction to create dot marking array on Si wafer. Two pulsed laser power applied were 25.5W and 39.6W to produce pattern, then immersed in 10% KOH solution to etch laser-induced structure and debris to form partial transparent Si wafer. Low power laser was induced 80-85 µm depth of micro-hole, while high power was induced 140-145 µm. KOH treatment was conducted to etch laser region which to form deeper and wide micro-holes. The bifacial solar cells have been fabricated using partial transparent Si wafer and the current-voltage of the devices were tested. The front surface efficiency obtained for both partial transparent bifacial solar cells were 4.36% and 5.59%, while rear surface achieved 1.23% and 1.16%. Fabricated conventional bifacial solar cell has an efficiency of 2.39% for front and 0.64% for rear. The surface modification enhanced the efficiency due to the photon path length transmission to rear surfaces, micro-hole's dimension and optical absorption in the near-infrared region.

Keyword: Bifacial solar cell; Surface modification; Pulsed laser; Efficiency; Partial transparent

INTRODUCTION

Solar cell become major technology in today's global harvesting clean and renewable energy as a substitute of fossil fuel-based energy sources (Basher et al. 2018). Performance progress has been made in improving the quality with low manufacturing cost. Therefore, two options have been discovered to improve the cell performance at low cost which are reducing Si wafer thickness we have engaged in a detailed analysis of manufacturing costs for each step within the wafer-based monocrystalline silicon (c-Si(Goodrich et al. 2013) and having bifacial surface for energy generation from both sides. In current market, Si wafer thickness is 180-200 µm. In this paper, *p*-type <100> crystalline silicon wafer with thickness of 200 µm and resistivity 1-3 Ω-cm were used to fabricate bifacial solar cell. Utilization thin wafer approaching fundamental limit caused by a thermal expansion mismatch between aluminum (Al) paste and Si wafer (Desa et al. 2016).

Bifacial solar cell has symmetrical configuration contacts on front and rear surface that able to eliminate expansion mismatch, decrease metal usage and improve photon absorption (Sepeai et al. 2013). Symmetrical configuration scheme increases short circuit current density (J_{sc}) of the device, which boost efficiency conversion due incident light absorb from the rear surface. In bifacial solar panel, transparent space between adjacent solar cell allows sunlight to transmit to rear surface. An appropriate designed reflector is installed on back surface panel in order to harvest incident light toward rear side of the device (Jakobsen et al. 2016). Reflector will lead to output enhancement of bifacial solar panel, although at larger panel. The limitation of this circumstances on bifacial solar panel able to be eliminated by developing special designed partially transparent bifacial solar cell to optimize light trapping on rear surface.

In order to optimize light trapping, typical pyramidal texture was developed through wet chemical etching using chemical bath alkaline solution (Al-Thani et al. 2016) for both sides. Pyramidal structure reduce light reflection of Si wafer to 11±0.2% in the wavelength of 550-840 nm (Al Ammar & Lahlouh Bashar 2017) compare to planar surface. Si wafer with planar surfaces reflected 30% of sunlight due to high refractive index in the visible spectral region (Gupta, & Carlson 2015). Thus, texturing surface able to produce high short-circuit current density (J_{sc}) and increase efficiency conversion per cell (Lee et al. 2018).

Surface modification through pulsed laser interaction can be considered as an alternative for reducing the light reflection on Si wafer surface. Surface modification by pulsed laser on textured wafer reduce surface reflectance through melting, ablation, and recrystallization (Paul et al. 2015). The pulsed laser wavelength 1064 nm was chosen, corresponding to a photon energy near the bandgap of Si which is 1.1 eV. Based on its wavelength, laser radiation is either fully or partially absorbed in the material. Laser-material interactions will lead either to local heating through electronic excitation or by electron-phonon coupling (Hamid et al. 2018). The absorption coefficient of Si becomes narrow towards the near infrared region (Battaglia et al. 2012). In the interest of environment- friendliness as well as inexpensive manufacturing, use of phosphoric acid (H_3PO_4) as the dopant source represents an almost perfect alternative as emitter dopant (S. Ahir et al. 2018).

In this paper, surface modification has been conducted by two pulsed laser power to produce dot marking with diameter of 0.5 mm and 2 mm distance as partial transparent Si wafer. The bifacial solar cell structure of n^+pp^+ with aluminum back surface field on partial transparent configuration were fabricated to investigate the performance output of current-voltage and efficiencies.

METHODOLOGY

Bifacial solar cell fabrication process has been shown in Figure 1. Figure 2 shows the n^+pp^+ bifacial solar cell on partial transparent Si wafer. The p-type <100> Si wafer with a sheet resistivity in a range of 1-10 ohm/cm were used. Si wafer was initially cleaned by directly immersed in 10% sodium hydroxide (NaOH) solution for 15 minutes to remove impurities and saw damage. After damage removal, the wafers were dip inside texturing solution for 30 minutes at 70^{o}C. After texturing process, the Si wafers were patterned by YMS-50D Semiconductor Laser Scribing Machine at laser power of 23.5W and 39.6W. This process was conducted at 15 kHz pulse frequency. Next, the Si wafer went through etching process using 10% potassium hydroxide (KOH) solution at 50^{o}C for 30 minutes to form partially transparent surface on patterned Si wafer. The process was conducted under low temperature which is 50^{o}C to prevent texturing surface diminished. High temperature KOH etching process expected to remove pyramidal texturing surface and reduce thickness of the Si wafer below 100 µm. The wafers were then subjected to the n^+ layer diffusion by dipping the patterned Si wafer into the 10% phosphoric acid (H_3PO_4) for emitter layer formation. Then Si wafers were annealed in quartz furnace tube at 875^{o}C for 30 minutes. For the Al-diffused p^+ layer formation, the Al pastes were screen-printed on back side of the patterned Si wafer and front dried at 150˚C for 10 minutes, then fired at 800˚C in a quartz tube furnace. Excess Al was removed by soaking in solution of hydrochloric acid (HCl) and hydrogen peroxide (H_2O_2) with a ratio of 50:50 to formed Al-BSF. After that, the oxide passivation process performed at 1000^{o}C for 30 minutes in a furnace to form anti-reflecting coating (ARC) and passivation layer.

Finally, the metallization processes were done by silver (Ag) and silver/aluminum paste (Ag/Al) printing using identical grid masks on a front and back surfaces of patterned Si wafer, respectively. Screen-printed contacts were fired at ~ 800˚C to form front and back contacts. The edges of Si wafers were then mechanically diced to achieve edge isolation. In order to analyze the performance of the devices, three main characterization processes were investigated, namely (i) cross section images of modified surface on Si wafer using Supra 55VP field emission scanning electron microscopy (FESEM) system, (ii) the IR transmission of the partial transparent Si wafer using IR Transmission Measurement System and (iii) current-voltage measurement of completed partial transparent bifacial solar cell using Light Current-Voltage (*I-V*) measurement system.

RESULTS AND DISCUSSION

Bifacial solar cell commonly developed pyramidal texture on front and rear side on Si wafer to enhance optical absorption by light trapping effect in fabrication process (Frank et al. 2012). Figure 3 shows top view image of pyramidal texture that was formed by wet-chemical method. Size of each pyramid structure was 2 -10 µm. This textured Si wafer were used for standard bifacial solar cell as a benchmark to be compared with partial transparent bifacial solar cell. The laser process also been done on pyramid textured surface.

Two laser power that has been used in this study were 25.5 W and 39.6 W can be denoted as sample A and B. Figure 4 illustrates depth of hole after two power model laser interaction. Laser induced in sample A was 80-85 µm and sample B was 140-145 µm. During laser induced process on Si wafer, a total of 2401 laser dot marking was developed on 100 cm^2 Si wafer for each sample.

Figure 5 shows top view image of sample A and B after laser process and KOH treatment. It is observed that sample A with laser power of 25.5 W produced donut-shaped pattern. Meanwhile, sample B with the laser power of 39.6 W produced holes-shapes.

Figure 6 shows the light emitting observation for both sample A and B. When the light emitted to both samples, sample B produce higher brightness compared to sample A. The different brightness occurs when hole developed between two samples have different size of hollow path.

Figure 7 shows cross-sectional images of sample A and B. Sample A formed trench with depth of 44.23 µm and 57.62 µm. From the figure 7, there are Si melting and recrystallization due to the laser induction on Si wafer. Meanwhile, sample B produced 353.7 µm width of hole-shaped pattern. From both samples, it is observed that the pyramid texture pattern was remain after laser process and KOH treatment.

From these images, it can be concluded that Si wafer created internal three-dimensional texture which are front,

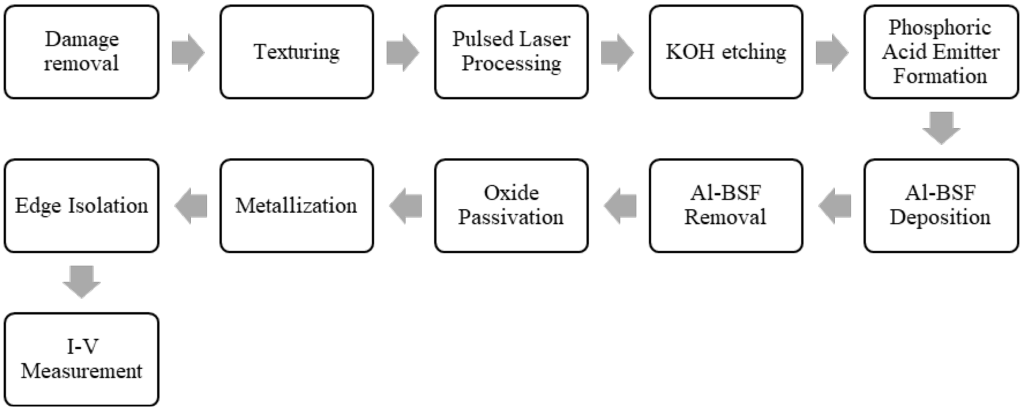

FIGURE 1. Bifacial solar cell fabrication process

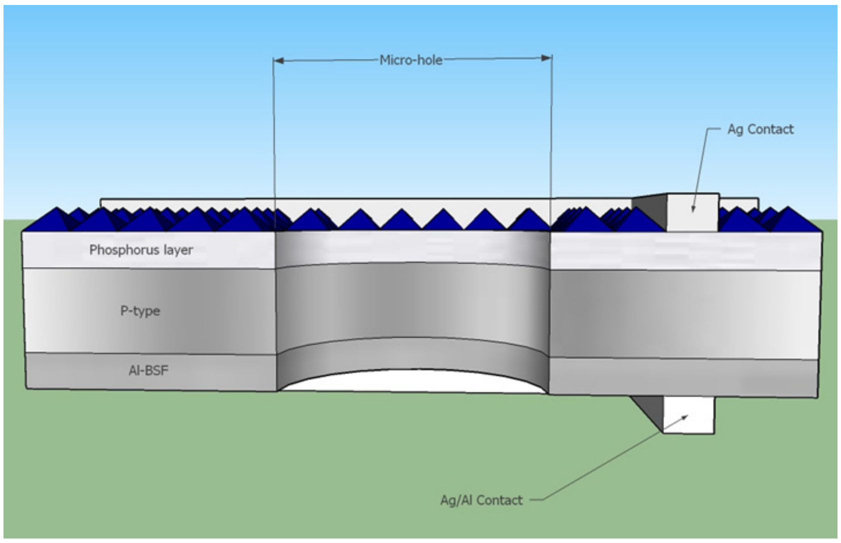

FIGURE 2. completed $n^{+}pp+$ solar cell cross-section

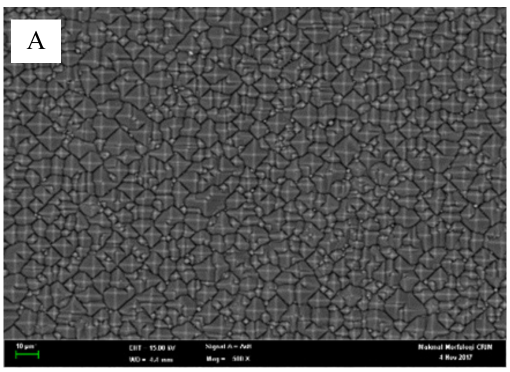

FIGURE 3. Top view images of pyramidal texture on Si wafer by FESEM with a magnification of 500X

rear and sidewall during surface modification using pulsed laser. The internal three-dimensional texture enhances surface optical absorption and increase near infrared transmission to backside region.

Figure 8 plots the transmission response in 900-1200 nm spectral range of sample A, B and C (without laser). From the graph, it is observed that sample A exhibited low transmission but still able to transfer light to backside region. Low transmission occurred when laser interaction creates surface roughness that responsible to enhanced absorption more on sidewall rather than transfer the light to backside region. It is noted that sample B has substantially higher transmission in comparison of sample A due to wider hole formed. Thus, more lights were able to pass through to backside region and increase optical absorption on rear side. Sample C with no modification with laser process and only textured surface shows the lowest transmission. Most of infrared transmission has been absorbed on front surfaces

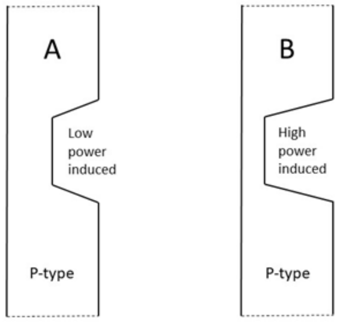

FIGURE 4. The illustration of depth of hole from two power model laser interaction

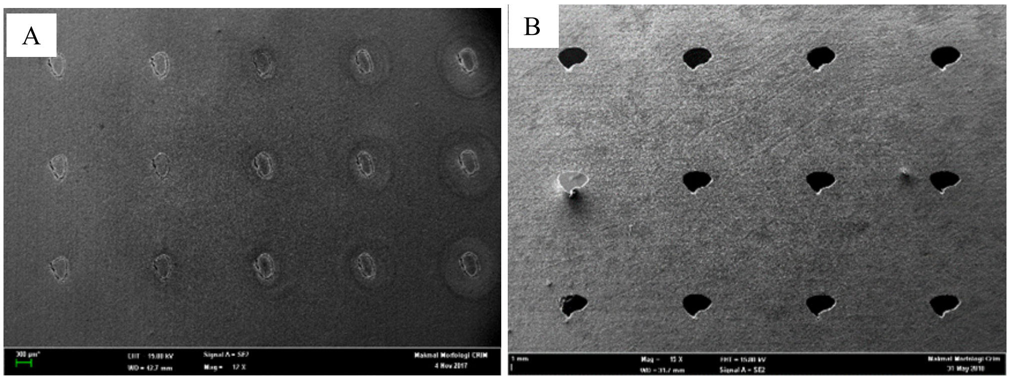

FIGURE 5. Top image of sample A and B

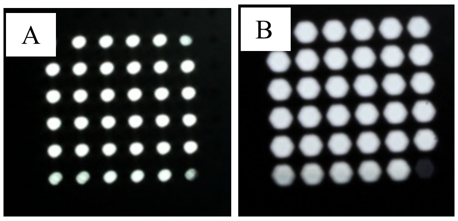

FIGURE 6. Light output from partial transparent Si wafer of (a) sample A and (b) sample B

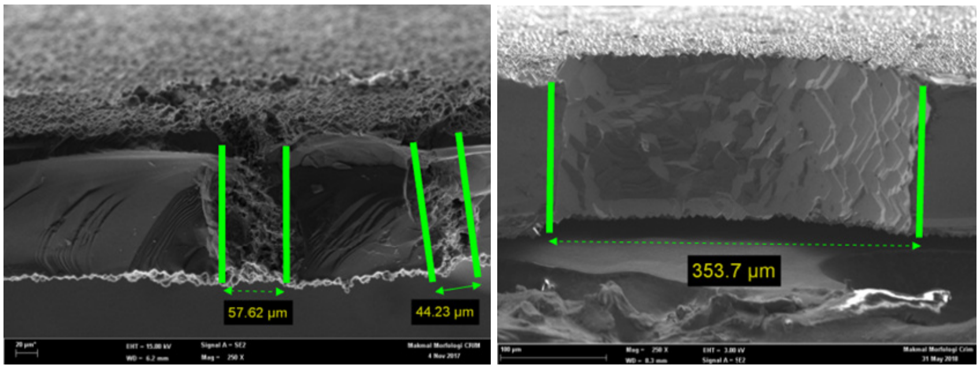

FIGURE 7. Cross-sectional FESEM view on sample A and B after KOH treatment

but transmission still occurs due to porous surface that may form during wet chemical process.

Partial transparent bifacial solar cells from donut-shaped and holes-shaped pattern Si wafer were fabricated. The sheet resistance produced were 27 Ω/sq and 48 Ω/sq. Figure 9 (a) and (b) plot current-voltage (I-V) measurement for sample A, sample B and sample C (without laser) for front and rear surface. Table 1 summarizes this result. All devices exhibited good performance under front illumination (n-p junction) than under rear illumination (p-p+ junction). The front surface efficiency obtained for sample A, B and C were 4.36%, 5.59% and 2.39%. While rear surface was 1.23%, 1.16% and 0.64%.

For front surface, open circuit voltage (V_{oc}) obtained, 546 mV,543 mV and 524 mV. The current densities are ~17.35 mA/cm^2,~20.14 mA/cm^2 and ~14.72 mA/cm^2

respectively. The increment of current density effects the efficiency of the devices by 1.23%. Besides width and depth of holes, enhancement of sheet resistance (R_{sheet}) of phosphorus doping also influence the J_{sc} measurement.

The improved efficiency of modified surface as partial transparent was due to the three-dimensional surface that occurred. By having three dimensional textured surfaces doped with phosphorus, photogenerated electron hole pairs contribute to J_{sc} due to recombination process has been reduced. Plus, the distance of minority carrier to travel become shorter. Even though incident light that of solar spectrum with photon energy (hv) on silicon wafer produce band-gap energy 1.12eV and weak absorption in 1-1.12 µm wavelength range, the modification surface able to improve the optical absorption.

For rear surface, open circuit voltage (V_{oc}) gained, 442 mV, 458 mV and 401 mV. The current densities are ~5.56 mA/cm^2, ~5.02 mA/cm^2 and ~4.2 mA/cm^2 respectively. The performance between device A and B has reduced 0.07% due to insufficient of back surface field. Efficiencies for all devices tested was quarter from front surfaces. Back surface field was made of layer of aluminum paste which annealing in furnace at 800^{o}C to form p^+ layer. Subsequently, it was removed by solution of HCl and H_2O_2 to reduce Al thickness. Thinner Al layer was created to increase minority carrier charge and simultaneously reduce the recombination rate on backside region. However, aluminum paste printed layer not aggressively enough annealing into Si wafer because phosphosilicate glass (PSG) was blocked Al to formed p^+ layer. Thus, annealing process resulted uneven layer of Al

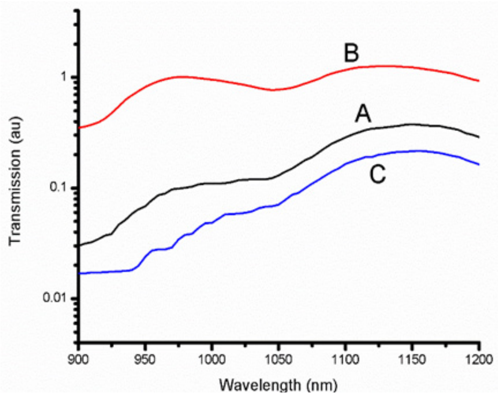

FIGURE 8. Optical IR transmission measurement as a function wavelength for sample A, B and C

TABLE 2. Comparison of bifacial solar cell performance of three devices.

Device	Surface	V_{oc} (V)	Jsc (mA/cm^2)	FF	P_{max}	η (%)	B (%)
A	Front	0.546	17.35	0.4145	0.3884	4.36	28.21
	Rear	0.442	5.56	0.45	0.1106	1.23	
B	Front	0.543	20.14	0.46	0.5031	5.59	20.75
	Rear	0.458	5.02	0.456	0.1044	1.16	
C	Front	0.524	14.72	0.3099	0.239	2.39	26.78
	Rear	0.401	4.2	0.38	0.064	0.64	

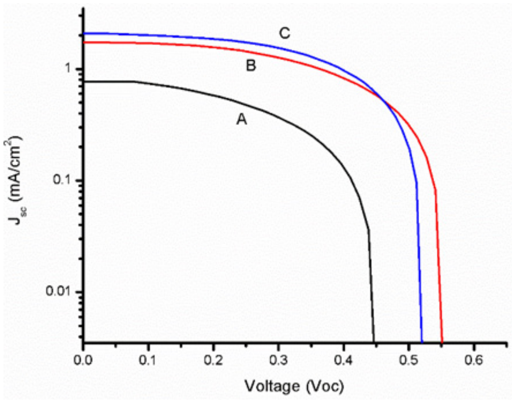

(a) Front

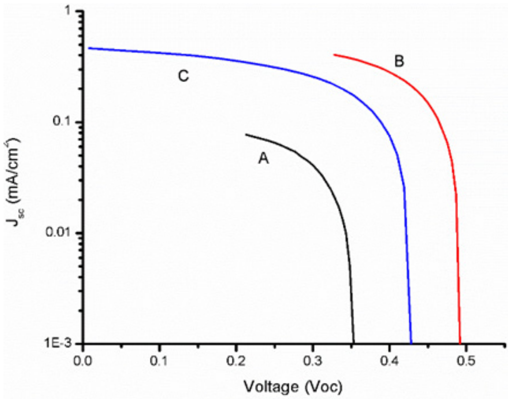

(b) Rear

FIGURE 8. LIV measurement of a typical bifacial solar cell for (a)front and (b)rear surfaces

after Al-BSF removal. Layer of PSG was ultra-thin glass layer that form after emitter diffusion. The present of glass layer on backside region cause Al remove easily with glass frit during removal process. The uneven Al layer generate low J_{sc} that cause by low minority carrier charge to generate electron-hole pairs and produce higher recombination. The efficiency for all sample was less than 1.3%. Low sheet resistance on backside region was inadequate to boost minority carrier charge which can be seen on figure 9(b). The plot data was incomplete to zero at y-axis and as a proof lack of optical absorption generated on rear side. Low efficiency of rear surface effect the bifaciality of the devices.

The bifaciality (B) parameter can be defined as the ratio of rear surface efficiency (η_{rear}) over front surface efficiency (η_{front}). This definition was based on the assumption of similar intensity of incident solar radiation on both rear and front surfaces (Ooshaksaraei et al. 2013).

According to bifaciality calculation in (1), bifaciality all devices can be increased by existence of an appropriate reflector which critical element to substantially increase optical absorption on rear surface. Besides that, rear surface fabrication needs to be improved by eliminate PSG layer to increase potential Al back surface field in generate high minority carrier charge and reduce recombination rate. The elimination of PSG also needs to be etched on front surface for reducing shading which blocked photon to be trapped in the devices.

CONCLUSION

Bifacial solar performance by using surface modification through pulsed laser interaction has been investigated. As a result, modification wafers possess an ability to improve the conversion efficiency through three-dimensional texturing which allow internal scattering in the sidewall which reduce travel distance of minority carrier and recombination rate. Through these, sample A with low energy laser induced Si wafer produced the efficiencies of 4.36% and 1.23% for front and back surface. While sample B with higher laser power produced the efficiencies of 5.59% and 1.16% for front and rear side. The efficiency for non-modified surface was 2.39% for front and 0.64% for rear. The three-dimensional texture from laser process enhancing light trapping for front surface. Poor performance on back surface due to Al paste prevented aggressively to anneal by phosphosilicate glass (PSG) layer. PSG layer recommended to be etched before Al printing to increase Al annealing surface and optical absorption rate. Low efficiency effected the bifaciality parameter of the devices. Real simulation under solar radiation with existence of reflector will be tested to increase performance of partial transparent solar cell especially of rear side

ACKNOWLEDGMENT

The authors would like to acknowledge RESTED 2018 that has provided a platform to present this work. This work has been carried out with the financially support of the Malaysia Ministry of Energy, Science, Technology, Environment and Climate Change (MESTECC) under Science Fund Project with a research code of 03-01-02-SF1322 and Universiti Kebangsaan Malaysia with GUP-2017-077 grant.

DECLARATION OF COMPETING INTEREST

None.

REFERENCES

Al-Thani, Hamda & Al-Jaeedi, Ahlam & Al-Shaibani, Sahar & Al-Yafeai, Abeer & Hasoon, Falah. 2016. The influence of texturing bath conditions on the morphology and optical properties of crystalline silicon. *PVSC (IEEE 43rd Photovoltaic Specialist Conference) 2016*, 100: 2844-2849.

Al, Ammar & Lahlouh, Bashar. 2017. Silicon Pyramid structure as a reflectivity reduction mechanism. *Journal of Applied Sciences* 17: 374-383.

Basher, Mohammad & Hossain, M. & Afaz, Romena & Tayyaba, Engr. Dr. Shahzadi & Akand, Rafiq & Rahman, Md & Eman, Nur Mohammad. 2018. Study and investigation of phosphorus doping time on emitter region for contact resistance optimization of monocrystalline silicon solar cell. *Results in Physics* 10: 205-211.

Battaglia, C., Boccard, M., Haug, F. J. & Ballif, C. 2012. Light trapping in solar cells: When does a Lambertian scatterer scatter Lambertianly? *Journal of Applied Physics* 112(9): 1–6.

Frank, J & Rüdiger, Marc & Fischer, Stefan & Goldschmidt, Jan Christoph & Hermle, Martin. 2012. Optical simulation of bifacial solar cells. *Energy Procedia* 27: 300-305.

Goodrich, Alan & Hacke, Peter & Wang, Qi & Sopori, Bhushan & Margolis, Robert & James, Ted & Woodhouse, Michael. 2013. Wafer-based monocrystalline silicon photovoltaics road map: utilizing known technology improvement opportunities for further reductions in manufacturing costs. *Solar Energy Materials and Solar Cells*, 114: 110-135.

Gupta, Mool & Carlson, David. (2015). Laser processing of materials for renewable energy applications. *MRS Energy & Sustainability*: *A Review Journal* 2: 1-15.

Poulsen, Peter & Jakobsen, Michael & Thorsteinsson, Sune & Rødder, Peter & Rødder, Kristin. 2016. Vertical reflector for bifacial PV-panels. *PVSC (IEEE 43rd Photovoltaic Specialist Conference) 2016*, 2678-2681.

Hamid, Siti & Sepeai, Suhaila & Zaidi, Saleem & Ahmad, Samir. 2018. Pulsed Laser Annealing of Ag-Paste on n-Doped Emitter. *Jurnal Kejuruteraan* SI1: 57-62.

Lee, Hyeon-Seung & Suk, Jaekwon & Kim, Hyeyeon & Kim, Joonkon & Song, Jonghan & Jeong, Doo Seok & Park, Jong-Keuk & Kim, Won & Lee, Doh-Kwon & Choi, Kyoung & Ju, Byeong-Kwon & Lee, Taek & Kim, Inho. 2018. Enhanced efficiency of crystalline Si solar cells based on kerfless-thin wafers with nanohole arrays. *Scientific Reports* 8: 3504.

Mat Desa, Mohd Khairunaz & Sepeai, Suhaila & Azhari, Ayu & Sopian, Kamaruzzaman & Amin, Nowshad & Zaidi, S.H.. 2016. Silicon back contact solar cell configuration: A pathway towards higher efficiency. *Renewable and Sustainable Energy Reviews* 60: 1516-1532.

Mohd Ahir, Z. F., Sepeai, S. & H. Zaidi, S. 2018. Optimization of Phosphoric Acid-Based Emitter Formation on Silicon Wafer. *Jurnal Kejuruteraan* SI1(3): 9-14

Ooshaksarei, Poorya & Sopian, Kamaruzzaman & Zulkifli, Rozli & Alghoul, Mohammad & Zaidi, Saleem. 2013. Characterization of a Bifacial Photovoltaic Panel Integrated with External Diffuse and Semimirror Type Reflectors. *International Journal of Photoenergy. 2013*

Sepeai, Suhaila & Leong, Cheow & Sopian, Kamaruzzaman & Zaidi, Saleem. 2013. Fabrication and characterization of Al-BSF bifacial solar cell. Conference *PVSC (IEEE 39th Photovoltaic Specialist Conference) 2013*, 2664-2668.

Verburg, P. C. 2015. Laser-induced subsurface modification of silicon wafers. Thesis PhD University of Twente, Enschede, The Netherlands.